Plant and Fungal Systematics 69(1): 85–98, 2024
DOI: https://doi.org/10.35535/pfsyst-2024-0009

ISSN 2544-7459 (print)
ISSN 2657-5000 (online)

Silicoflagellates and other siliceous micro- and nannofossils from Rupelian diatomites, southeastern Poland

Irena Kaczmarska[1*] & James M. Ehrman[2]

Article info
Received: 23 Jan. 2024
Revision received: 16 May 2024
Accepted: 21 May 2024
Published: 16 Jul. 2024

Associate Editor
Judita Koreiviene

Abstract. The Eocene-Oligocene Transition is one of the major stages of the Cenozoic reshaping of the world oceans with associated changes in climate, of ocean coastlines and circulation patterns. This altogether created challenging environments for fossilization and preservation of native biota. Consequently, well preserved Oligocene fossils are infrequent worldwide and just as rare in the Central Paratethys. The well-preserved Rupelian (Early Oligocene) diatomites from the Skole Nappe, the external unit of the Outer Carpathians in southeastern Poland were deposited in the Central Paratethys. In some samples, in addition to diatoms, sediments also contain a great diversity of other silicified micro- and nannofossils. Here we report our findings of silicoflagellates (fifteen taxa from five genera), two rotosphaeridians, and several morphotypes of fossil scales, some of uncertain taxonomic affinity. Among silicoflagellates, the most common are species from genera *Corbisema* (*C. triacantha*, *C. hastata*, and *C. apiculata*) and *Dictyocha* (*D. clinata* and *D. fibula*). We also recovered scales of rotosphaeridians (*Pinaciophora* and possibly *Rabdiophrys*) and remains of organisms of uncertain affinity (*Clathropyxidella* and *Macrora*) often reported together with silicoflagellates. All of these taxa are the first reports for the Central Paratethys. Silicoflagellate species composition is consistent with the datums derived from other fossils. Silicoflagellates, marine diatoms and archaeomonads suggest a neritic depositional environment.

Key words: Central Paratethys, *Clathropyxidella*, dictyochophyceans, Early Oligocene, *Macrora*, rotosphaeridians, siliceous nanoscales

Introduction

Extant dictyochophyceans (commonly called silicoflagellates) are a relatively small group of cosmopolitan marine planktonic microeukaryotes encompassing both silicified and non-silicified members, although in several genera cell walls may contain non-mineralized scales (Graham et al. 2008; Derelle et al. 2016). Their extracellular siliceous skeletons are structurally simple, generally in the form of a shallow basket in which the core of the protoplast resides. Silicoflagellate taxonomy is based on the structure of these skeletons. This allows common systematics for fossil remains and extant species. Genetic and cellular evidence places silicoflagellates as a sister to pelagophytes, both within the heterokonts (Burki 2014; Strassert et al. 2019). Their cells are equipped with a flagellum bearing mastigonemes, have ER chloroplasts and typically brown photosynthetic pigments (chlorophyll *a* and *c* together with accessory pigments fucoxanthin, diadinoxanthin, diatoxanthin, lutein, and β-carotene; Van den Hoek et al. 1995). Recently, molecular clock analyses indicated that the dictyophytes/pelagophytes clade shared the last common ancestor with their sister clade (bacillariophytes/parmaphytes) in the mid-Neoproterozoic (Strassert et al. 2021). These four well-known stramenopile lineages belong to a very diverse clade, TSAR (*Telonemia-Stramenopila-Alveolata-Rhizaria*; Tikhonenkov et al. 2022).

The extracellular silicified skeletal remains of silicoflagellates are known since at least the early Cretaceous (Haq 1998; McCartney et al. 2010). These remains were preserved even though most are constructed of interconnected thin, hollow tubular rods that are relatively susceptible to mechanical damage. As a group, they reached greatest species diversity in the Miocene with over one hundred species, but have since declined to one or a few extant genera. Altogether, approximately 24 fossil silicoflagellate genera are recognized in Desikachary & Prema (1996), but the exact number depends on taxonomic treatment. Silicoflagellates are used in biostratigraphy due to their presence in sediments where other microfossils are scarce and to their fidelity to relatively cool waters

---

[1] Biology Department, Mount Allison University, Sackville, New Brunswick, E4L 1G7, Canada
ORCID: 0000-0002-2527-6148
[2] Digital Microscopy Facility, Mount Allison University, Sackville, New Brunswick, E4L 1G7, Canada
ORCID: 0000-0001-7428-2651
[*] Corresponding author e-mail: iehrman@mta.ca

(McCartney 1993; Desikachary & Prema 1996; Graham et al. 2008). In sediments containing fossilized silicoflagellates, other siliceous remains are often present as well. Some of them are of uncertain taxonomic identity, either because they have not yet been found associated with an entire organism or differ from known taxa in some way. *Macrora* and *Clathropyxidella* are examples of such microfossils. They are widely distributed and reported from many silica-rich sediments together with diatoms and/or silicoflagellates. Other enigmatic fossilized remains include various siliceous scales. For example, *Hyalolithus*, originally found in fossilized form, was recently tied to an unusual, silicified haptophyte (Abe et al. 2016, 2022). It is therefore possible that other, yet undetermined protists might have also produced silicified micro- and/or nannofossils left behind in ancient sediments (Bessudova et al. 2022; Siver & Lott 2023).

Here, for the first time we report on Rupelian silicoflagellates, *Macrora*, *Clathropyxidella*-like fossils, and scales reminiscent of various other microeukaryotes. All were found in samples together with well-preserved diatoms, parmaleans, ebridians, archaeomonads and sponge spicules in diatomites or diatom-rich sediments deposited in the Central Paratethys, now in southeastern Poland. When justifiable, we place these fossils in their paleoenvironmental context.

Materials and methods

Sedimentary and stratigraphic setting

Diatom-rich sediments and diatomites from the Skole Nappe, the external unit of the Outer Carpathians in southeastern Poland, occur mostly in early Oligocene and early Miocene strata (Kaczmarska 1982; Kotlarczyk 1982; Kotlarczyk & Kaczmarska 1987; Kotlarczyk & Lesniak 1990). The lithostratigraphy and composition of the other associated siliceous microfossils in examined samples from the Futoma Horizon, the lower part of the Menilite Formation of this Nappe is radiometrically dated as Rupelian (28.9 ± 1.2 Ma) within a calcareous nannoplankton zone NP23/24-NP24 (Kotlarczyk et al. 2006; Kotlarczyk & Uchman 2012). Regional paleogeography of the Paratethyan realm during the Oligocene may be found in Picha & Stranik (1999), Kotlarczyk & Uchman (2012), and Sachsenhofer et al. (2017). The evolution, paleogeography, and paleoceanography of the entire Paratethys is reviewed in Palcu & Krijgsman (2023). All recent paleoceanographic reconstructions converge on a relatively isolated sea with at times reduced salinity and anoxic deeper waters. The Central Paratethys had only limited and temporary connection and water exchange with the North Sea, the Western Paratethys, and the Eastern Paratethys.

The Lower Oligocene diatomites and diatom-rich shales are widely distributed in southeastern Poland (Kotlarczyk 1982; Kotlarczyk & Lesniak 1990). Early investigations identified only the most common diatom species in the Futoma Horizon (Kaczmarska 1982; Kotlarczyk & Kaczmarska 1987). More current additions to the diatom and parmalean species composition may be found in Kaczmarska & Ehrman (2008, 2023). Native silicoflagellates are associated with a diverse assemblage of mostly shelf-sea diatoms such as *Rhizosolenia*, *Chaetoceros* (frustules, spines, and spores), *Paralia*, *Hyalodiscus*, *Actinocyclus*, and several genera from the orders *Cymatosirales* and *Hemiaulales*. In addition, some heavily silicified non-raphid (fragillarioid) and raphid (achnanthid, cocconeid, amphorid) taxa are also well represented. In some samples there is also a considerable diversity and quantity of archaeomonads. Such fossil species composition suggests a marine, but not an open ocean, environment (Kotlarczyk & Kaczmarska 1987; Kotlarczyk et al. 2006; Kotlarczyk & Uchman 2012) with a detectable periodic contribution of less saline waters.

Field work and laboratory processing

Samples for this study were collected from outcrops near the villages of Futoma (49.860°N, 22.132°E), Hermanowa (49.941°N, 22.020°E), Borek Nowy (49.932°N, 22.085°E), and Łubno (49.820°N, 22.167°E) in southeastern Poland. Their locations are shown in Kotlarczyk & Kaczmarska (1987). The state of preservation of the fossilized remains differed from sample to sample. Therefore, in this report only the best preserved and most diverse samples from various sites were chosen for in-depth examination. These included: Futoma (samples 4, 13, 14, 16, 17, 18), Hermanowa (samples 23, 27), Borek Nowy (samples from Dom 5, 6, 12, and Kawalec), and Łubno (samples 3, 4).

Sediments were processed for microscopy as described in detail in Kaczmarska & Ehrman (2023). Briefly, sediments were soaked in distilled water to loosen aggregates and then treated with 3–10% HCL to remove calcareous components, rinsed with distilled water, boiled in 5% sodium carbonate and 30% H_2O_2, cooled, then rinsed repeatedly with distilled water to remove most of the clay particles. Lithified samples were disaggregated with boiling 10% KOH or NaOH. For light microscopy (LM) cleaned fossils in distilled water were deposited onto glass coverslips, air dried and mounted in Zrax (refractive index 1.7+, Prof. W. Dailey formula) and examined using a Zeiss upright microscope (VEB Carl Zeiss Jena, East Germany). Camera lucida sketches or outlines made from tracing LM images were created when sediments or other debris made details difficult to discern in photographs. Preparation for scanning electron microscopy (SEM) involved depositing cleaned fossils in distilled water onto 1 μm pore size PTFE filters in a Millipore vacuum filtration apparatus. Dried filters were mounted on aluminum support stubs, sputter coated with gold and examined using a Hitachi SU3500 SEM (Hitachi High-Technologies Canada, Inc., Etobicoke, Ontario, Canada) operating at 10 kV and 5 mm working distance. The entire SEM stub surface was transected using at least 1000× magnification for less species-rich samples while one half of the stub was examined for samples where microfossils were abundant. Skeletal terminology used for silicoflagellates follows Bukry (1976c), Onodera & Takahashi (2009), and McCartney & Witkowski (2016). Named skeletal elements of representative silicoflagellate genera are illustrated in Abe et al. (2015) and McCartney et al. (2022).

Results

Fifteen taxa from five genera of silicoflagellates, two rotosphaeridians, and several other morphotypes of siliceous micro- and nannofossils, some of uncertain taxonomic affinity were found in 14 samples from 5 sites (Figs 1–4). Measurement ranges including a value in parentheses indicate an outlier. In some species more than one incomplete specimen was used for measurements of characters, thus some characters are reported with a single measurement. Occurrence ranges for the silicoflagellate species presented below are given in Table 1.

Bachmannocena quadrangula (Ehrenberg ex Haeckel) Bukry (Fig. 1A)

Description. Basal ring rhomboidal with spines at each corner. Major axis 33.7 µm, minor axis 28.4 µm long. Basal spines 11.3–17.3 µm long, longer spines aligned with major axis of basal ring. No apical apparatus.

Notes. Our specimens align with the description and size given for the species described by Desikachary & Prema (1996). Other workers also illustrate rhomboidal basal rings and spines of unequal length (as *Mesocena quadrangula* Haeckel; Bukry 1980, 1983; Bukry & Monechi 1985; Martini 1990) attesting to variability of metrics among the skeletons of this species. *M. elliptica* (Ehrenberg) Ehrenberg shown in Desikachary & Prema (1996) demonstrate a few rhomboidal specimens, but their apical spines are significantly shorter relative to the basal ring when compared to those in our specimens.

Occurrence. Borek Nowy Dom 12.

Corbisema apiculata (Lemmermann) Hanna (Fig. 1B–C)

Description. Basal ring sides nearly equilateral. Majority of struts are as wide as the basal ring sides and divide it into three sections. Basal sides 17–40 µm long. Basal spines short, 0.4–3.5 µm long. Pikes present, inwardly curved and emerging slightly off the center of the struts base.

Notes. Tsutsui et al. (2018) conducted an extensive morphometric analysis of the specimens from the Eocene *C. apiculata-C. triacantha* (Ehrenberg) Frenguelli species complex. They proposed metric characters that could be most helpful in separating these two species. They concluded that *C. apiculata* sensu stricto (s.str.) has relatively short basal spines compared to *C. triacantha*. Their *Corbisema apiculata* was comprised of two subgroups, B1 and B2. Only B1 possesses pikes, as do our early Oligocene specimens. The metrics found in their specimens were 28–78 µm for the basal ring sides and 3–18 µm for spines, thus overlapping with our specimens. Skeletons illustrated in Tsutsui et al. (2018) are the most similar to our specimens in overall basal ring outline and side-to-spine proportions. *Corbisema apiculata* f. *minor* (P. Schulz) Harwood is overall smaller with the basal sides 15–20 µm long and very short basal spines (Glezer 1970), thus smaller than all but a few of our specimens.

Larger specimens are shown by Desikachary & Prema (1996) with 50–130(30) µm long basal ring sides and basal spines up to 15 µm long, thus larger than our specimens. Similarly, Loeblich et al. (1968) and Glezer (1970, as *Dictyocha triacantha* var. *apiculata* Lemmermann) also report larger skeletons with basal sides 51–130 µm, and spines from barely visible to 15 µm long.

Occurrence. Futoma 4, 17, 18, Borek Nowy Dom 12, Borek Nowy Kawalec.

Corbisema cf. ***geometrica*** Hanna (Fig. 3A)

Description. One complete specimen found with widely rounded, triangular outline, convex sides, 19–23 µm long and 27 µm wide. Partially damaged specimens added to metrics of the basal ring sides which varied from 24–38 µm long. Three struts join basal ring in slight indentations, as thick as ring sides. Minute apical spines

Table 1. Occurrence ranges of silicoflagellate species found in this study.

Species	Occurrence range	Sources
Bachmannocena quadrangula	Cretaceous – Recent	3, 5
Corbisema apiculata	Late Cretaceous – Recent	3, 4
C. geometrica	Late Cretaceous – Early Oligocene	3
C. hastata	Early Paleocene – Pliocene	3, 4
C. hastata subsp. *minor*	Late Paleocene – Oligocene	3
C. triacantha	Early Cretaceous – Quaternary	3
C. triacantha var. *nuda*	Middle Miocene	3
Dictyocha clinata	Middle Eocene – Pliocene	3
D. deflandrei	Early Eocene – Late Oligocene	1, 2, 3
D. fibula	Late Cretaceous – Recent	3
D. fibula subsp. *angusta*	Late Eocene/Early Oligocene – Late Pliocene	3
Distephanopsis crux	Late Cretaceous – Recent	3
Neonaviculopsis eobiapiculata	Paleocene – Late Oligocene	2, 3

Sources: 1 – Bukry (1976b); 2 – Bukry (1991); 3 – Desikachary & Prema (1996); 4 – Lozar & Mussa (2003); 5 – McCartney et al. (1995).

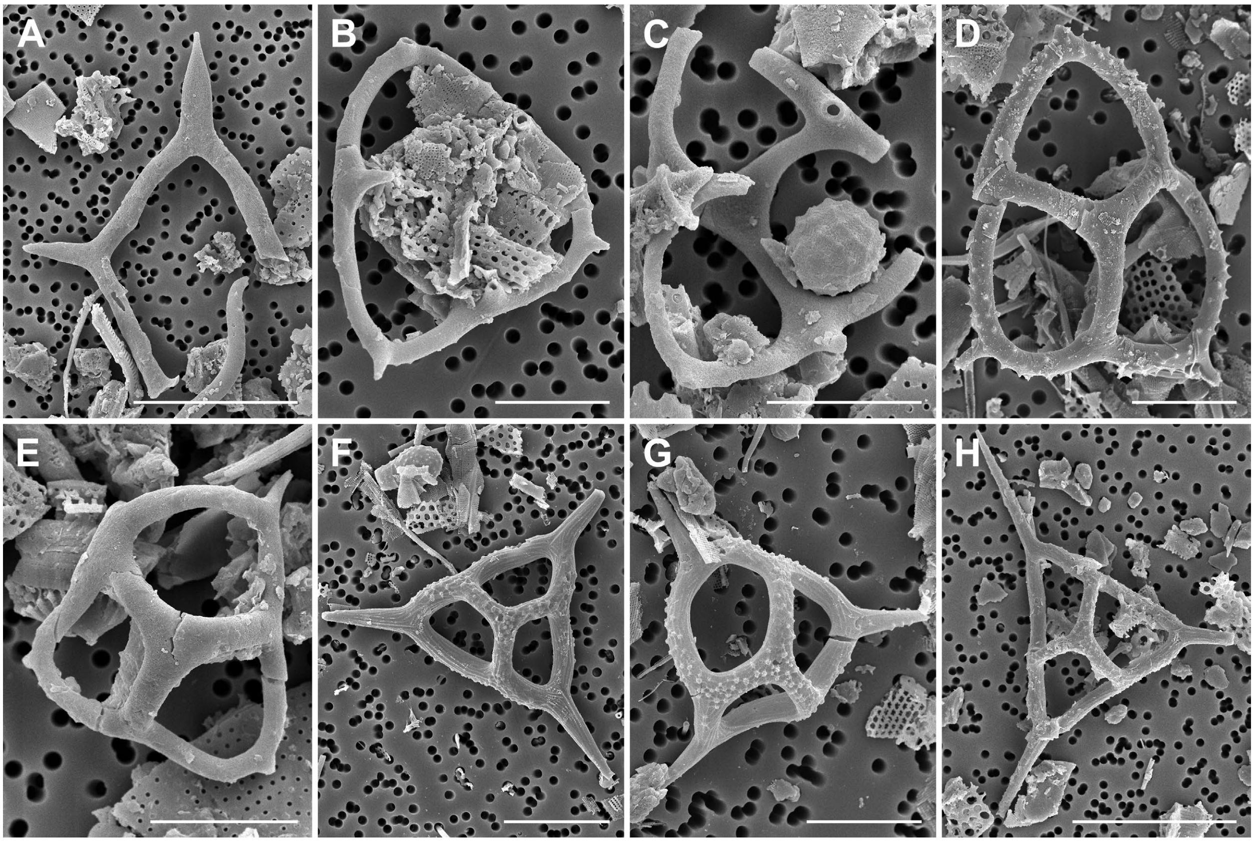

Figure 1. SEM images of silicoflagellate skeletons. A – incomplete skeleton of *Bachmannocena quadrangula*; B – partially obscured skeleton of *Corbisema apiculata*, note short apical spines and pikes at junction of struts with basal sides, tips of two pikes broken off; C – incomplete skeleton of *Corbisema apiculata*, note shape of struts; D – slightly tilted specimen of *Corbisema hastata*; E – apical view of *Corbisema hastata* subsp. *minor*; F – *Corbisema triacantha* with apical spines of average length, the most common morphotype in our material; G – *Corbisema triacantha* illustrating domed struts; H – *Corbisema triacantha* with long apical spines, a less common morphotype in our material. Scales: A, H = 25 µm; B–G = 10 µm.

present on some specimens. Neither apical plate nor pikes were seen.

Notes. Our specimen is most similar to those shown by Shaw & Ciesielski (1983), which contrary to many illustrated by other authors (e.g., Desikachary & Prema 1996) carry minute apical spines, but not an apical plate.

Occurrence. Futoma 14.

Corbisema hastata (Lemmermann) Frenguelli
(Fig. 1D)

Description. Basal rings isosceles with relatively straight minor side and scalloped major sides. Major basal sides 30–45 µm long, minor sides 22–35 µm long. Longest preserved basal spines 3.0–4.3 µm long and two aligned with major axis of skeleton. Small pikes found on some skeletons.

Notes. Similar to our specimens, Desikachary & Prema (1996) show skeletons with major basal ring sides 25–52 µm long, minor side 24–30(40) µm long, and spines of varied length, from minute up to 14 µm long. Glezer (1970) presented this taxon as one of several varieties of *Dictyocha triacantha* Ehrenberg and shows similar range of sizes, with basal ring major sides 27–52 µm and the minor side 15.3–40 µm long. Onodera & Takahashi (2009) also illustrate nominal and other varieties with a considerable range of skeleton sizes and ring shapes.

Occurrence. Łubno 4, Borek Nowy Dom 5, Borek Nowy Kawalec.

Corbisema hastata subsp. ***minor*** (P. Schulz) Bukry
(Figs 1E, 3B)

Description. Basal rings isosceles with straight minor side (17.3 µm long) and convex, rounded major sides (17.8–19.1 µm long). Longest preserved basal spines up to 2.5 µm long, at least some aligned with major axis of skeleton.

Notes. Our specimens meet the criteria for the size of this subspecies and are most similar to those shown by Glezer (1970), Bukry (1975a), and Onodera & Takahashi (2009).

Occurrence. Borek Nowy Dom 12.

Corbisema aff. ***hastata*** subsp. ***globulata*** Bukry
(Fig. 3C)

Description. Single specimen found has isosceles outline, deeply lobated sides, and short basal spines (longest 4.9 µm), major basal side 41.3 µm, maximal extent of short axis 37.3 µm, located above minor basal side. Minor basal side approximately 22 µm long. Struts delicate, thickness equal to basal ring.

Notes. The isosceles outline of the basal ring aligns with the diagnosis of *Corbisema hastata* subsp. *globulata*. However, the scalloping of the basal ring is more pronounced in our specimen than typically shown for this subspecies (Bukry 1976a; Shaw & Ciesielski 1983; Onodera & Takahashi 2009). The basal ring of our specimen gives the impression of three separate ellipsoidal components sharing part of their internal sides. Nonetheless, the original description emphasizes lobated sides of the basal ring as an important diagnostic character. In this specific character our specimen is also reminiscent of *C. archangelskianum* (P. Schulz) Frenguelli, *C. geometrica*, *C. inermis* subsp. *ballantina* Bukry, *C. katharinae* Bukry, *C. ovalis* K. Perch-Nielsen, and *C. toxeuma* Bukry. However, in all but one of these species the basal ring is equilateral and/or they lack apical spines.

Occurrence. Futoma 13.

Corbisema triacantha (Ehrenberg) Frenguelli (Figs 1F–H, 2A)

Description. Equilateral basal rings with well developed apical spines. Basal ring sides vary from slightly concave to slightly convex, 19.5–27.0 μm long. Spines 9.6–14 μm long. Three struts arch up and join above basal ring plane, attaching at about mid-distance between ring corners. No pikes found.

Notes. Tsutsui et al. (2018) conducted a morphometric analysis of the Eocene specimens of the *C. apiculata-C. triacantha* species complex and found that the basal ring side to spine ratio is a character helpful in distinguishing the two species. The basal spines are relatively longer with respect to ring sides in *C. triacantha* than in *C. apiculata*, as can be seen in our specimens. Best preserved specimens in our material fall near the lower range of species-specific sizes. Similarly, Desikachary & Prema (1996) report skeletons with 23–56(18) μm long basal ring sides and spines 10–22(3) μm long while Glezer (1970) found specimens with 18–56 μm long basal sides and 3–22 μm long basal spines.

Under the name *C. triacantha* var. *fexuosa* Stradner from the Chattian Stage of Oligocene deposits from Austria, Loeblich et al. (1968) illustrated specimens with an apical plate and a range of spine-to-ring base ratios. The variety was later elevated to species status (Perch-Nielsen 1975) emphasizing diagnostic significance of the concavity of the basal ring sides and asymmetric orientation of the struts. None of our specimens carry an apical plate. Most of our specimens do not show concavity of the ring sides as strong as indicated in the original description, but some do show asymmetric positioning of the apical apparatus.

Occurrence. This is the most common species in our samples. It was found in Futoma 4, 14, 17, Borek Nowy Dom 5, 6, 12, Borek Nowy Kawalec, Łubno 4, Hermanowa 27.

Corbisema triacantha var. ***nuda*** Bukry (Fig. 2B)

Description. Skeletons with triangular, equilateral basal ring, 20–22 μm long sides. Spines located at corners of basal ring and perpendicular to opposing side, approximately half the length of the side, 10–11 μm long when undamaged. Vestigial struts not discernible.

Notes. Our specimens show immediate affinity to *C. triacantha* in skeleton morphology and size, as already noted by Bukry (1982). In the original material, vestigial struts vary in size and number, and include specimens where vestigial struts are absent.

Occurrence. Borek Nowy Dom 12.

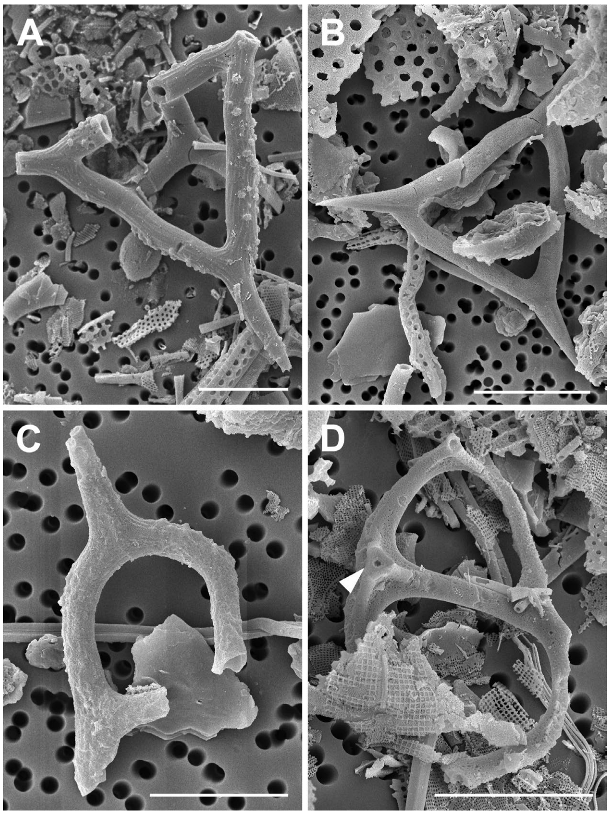

Figure 2. SEM images of silicoflagellate skeletons. A – *Corbisema triacantha*, basal side showing the absence of pikes; B – *Corbisema triacantha* var. *nuda*; C – partial skeleton of *Neonaviculopsis* cf. *eobiapiculata* preserving only one of two portals; D – slightly damaged specimen of *Neonaviculopsis* sp. aff. *N. neonautica* var. *cocosensis*, note minute apical spines and broken off pike (arrowhead). Scales: A–D = 10 μm.

Dictyocha clinata (Bukry) McCartney, Churchill, and Woestendiek (Fig. 3D)

Description. Basal rings with rounded rhomboid outline, 32.0–46.3 μm in long, 28.3–36.3 μm in minor axis with basal sides 19–26 μm long. Two long and two shorter apical spines, 17–26 μm and 10.0–14.6 μm long, respectively. Apical bar elevated above basal ring and inclined respective to its minor axis.

Notes. Morphology of our skeletons display characters diagnostic for this species (rounded rhomboid outline, spines of different length, and elevated and inclined apical

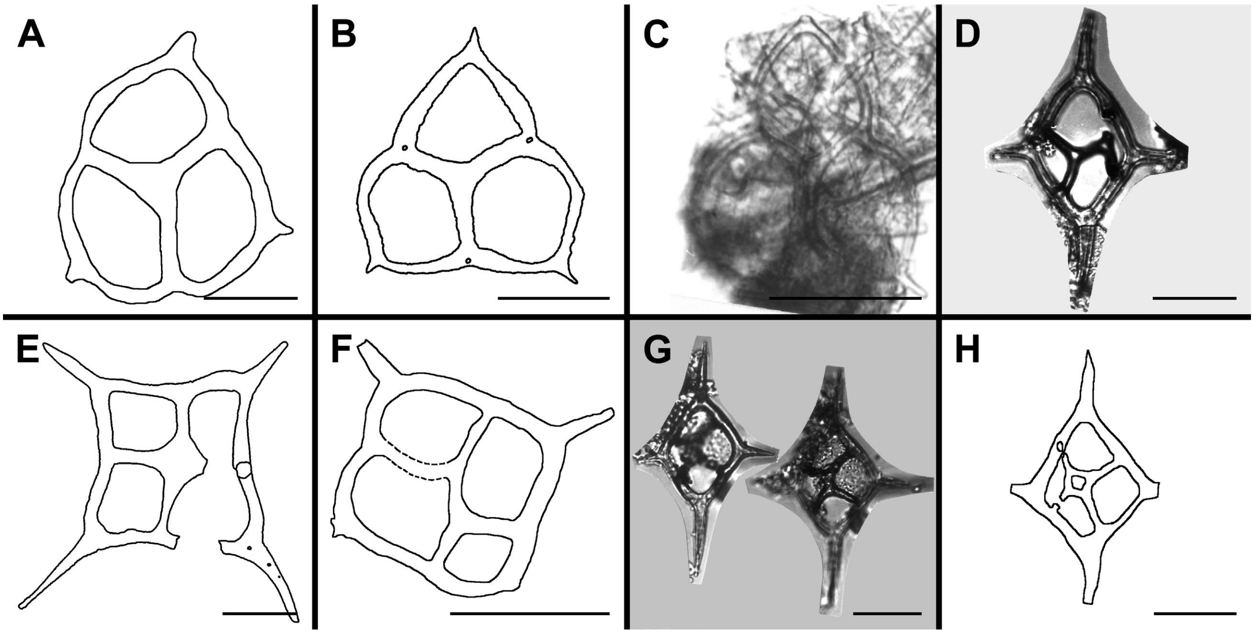

Figure 3. LM images, tracings of LM images, and camera lucida line drawings of silicoflagellate skeletons. Dashed lines indicate uncertainty due to features obscured by sediments or debris. A – *Corbisema* cf. *geometrica*; B – basal view of *Corbisema hastata* subsp. *minor*, with minute pikes; C – *Corbisema* aff. *hastata* subsp. *globulata*, note nearly elliptical portals and equally delicate struts and sides of basal ring; D – *Dictyocha clinata*, note inclined apical bar; E – slightly broken skeleton of *Dictyocha deflandrei*; F – *Dictyocha fibula* incomplete skeleton; G – *Dictyocha fibula* subsp. *angusta*, two images show the same skeleton at different focal planes; H – *Distephanopsis crux* s.lat. Scales: A–B, E = 10 µm; C–D, F–H = 25 µm.

bar) that separate it from *D. aspe*ra (Lemmermann). However, their sizes are near to or slightly below the minimum skeleton size range given by Bukry (1975b).

A species with a similarly canted apical bridge, *D. byronalis* Bukry, differs from our specimens by having "bowed-out" sides at the asymmetric struts-junction, which can produce a nearly eight-sided basal ring outline, and the absence of distinct pikes (Barron et al. 1984). Another somewhat similar species, *Dictyocha subclinata* Bukry, was disregarded based on the difference in length between the major and minor axial spines. The minor spines should be 3–12 times shorter than the major spines in these and other documented specimens of *D. subclinata* (Locker & Martini 1986; McCartney et al. 1995). In contrast, minor spines on our specimens are always less than 3 times shorter than the major ones. As well, our specimens are overall somewhat smaller, with the basal rings 32–46 µm long, versus 45–56 µm in *D. subclinata*. Finally, *Dictyocha concavata* Dumitrică differs in its basal ring shape which is expected to be "squarish or rhombic" with slightly concave sides, thus different from our specimens which are not concave. No skeletal dimensions were given by Dumitrică (1978).

Occurrence. Futoma 14, 16, 17, 18, Borek Nowy Dom 12, Hermanowa 23.

Dictyocha deflandrei Frenguelli ex Glezer (Fig. 3E)

Description. Only one specimen was found. Basal ring nearly square, straight to slightly concave sides, 20–22 µm long. Four basal spines of nearly equal length, 8–13 µm long. Struts perpendicular to ring sides, joining a large and square apical bar. Portals equal in size.

Notes. Glezer (1970) describes and illustrates this taxon and its varieties. The nominal variety has basal ring sides 18–25 µm long and spines 6–15 µm long, thus in agreement with our specimen. Also, the specimens from Onodera & Takahashi (2009) are very similar to ours in skeletal proportions, but somewhat larger (25–50 µm for basal ring diameter).

Occurrence. Futoma 4.

Dictyocha fibula Ehrenberg (Fig. 3F)

Description. Basal rings quadrangular with slightly convex sides, four relatively short basal spines, 10–19 µm long. Basal ring sides nearly equal in length (24–29 µm long). Portals unequal in size and pair of smaller and larger within the basal rings. Pikes not discernible in our material due to obscuring debris.

Notes. Glezer (1970) describes several forms and varieties and illustrates a great number of specimens, some with very small pikes. Desikachary & Prema (1996) show specimens with an even greater range of morphological variability, particularly the range of variation in portals. Ichikawa et al. (1967) illustrate skeletons with a more rectangular outline of basal rings and more variable length of spines and pikes. All of these authors comment on the plasticity of this taxon as the long list of synonyms and/or varieties attest (Ichikawa et al. 1967; Glezer 1970; Desikachary & Prema 1996). All may also represent a complex of morphologically similar species in need of taxonomic reappraisal.

Occurrence. Futoma 14.

Dictyocha fibula subsp. ***angusta*** Bukry (Fig. 3G)

Description. Basal ring in the form of an elongated rhombus with portals almost equal in size. Two basal spines (aligned with skeleton major axis) longer than the two others, 16–26 µm and 9–15 µm long, respectively. Apical bar aligns with major axis and long basal spines. Long basal spines about half the length of internal diameter of the basal ring. Basal ring 37–45 µm long and 24–42 µm wide. Pikes not discernible.

Notes. Similar specimens were also described as *Dictyocha fallacia* K.E. Busen and S.W. Wise although with lesser differences in length of basal spines, but similar in basal ring dimensions. However, Desikachary & Prema (1996) consider *D. fallacia* a conspecific with *D. fibula* subsp. *angusta*, even though the basal ring of their specimens are not rhombic and apical spines are nearly equal in length. *Dictyocha perlaevis* Frenguelli differs from our specimens by having bowed out ring sides and short apical spines while *Dictyocha messanensis* Haeckel illustrated in Martini (1982) differs by having a spine on the bridge of the apical apparatus.

Occurrence. Futoma 14, Łubno 4.

Distephanopsis crux s.lat. (Ehrenberg) Dumitrică (Fig. 3H)

Description. Rhombic basal ring with portals nearly similar in size and small apical ring. Basal spines unequal in length, two major spines significantly longer than other two. Basal ring 37–40 µm in major and 31–36 µm in minor axis, basal sides approximately 28 µm long. Apical ring 7–9.0 µm in largest linear dimension.

Notes. Recently, the genus *Distephanus*, where *D. crux* had been originally placed, was found to be invalid, and some species were transferred to *Stephanocha* (Jordan & McCartney 2015) and/or *Octactis* (Chang et al. 2017). This does not pertain to *D. crux*, which had been previously transferred to the then new genus *Distephanopsis* by Dumitrică (1978). Our specimens differ from the majority of specimens illustrated as *Distephanus crux* s.str. in less rounded outline of the basal ring and spines of slightly shorter length (Ichikawa et al. 1967; Glezer 1970; Locker & Martini 1986; McCartney & Wise 1987; Schellpeper & Watkins 1998). Many of these specimens seem to be smaller overall, although sizes are infrequently reported. In cases when they are given, they were close to or within the ranges we recovered (Glezer 1970; McCartney & Wise 1987; Desikachary & Prema 1996). *D. crux* is regarded as a polymorphic species, encompassing numerous varieties and forms, perhaps representing a complex of morphologically related species. Overall, with long and short apical spines and small apical ring, our specimens are most similar to *Distephanus longispinus* (Schultz) Bukry ex Foster (Bukry & Foster 1973, and other sources listed in Bukry 1978a) as *D. crux* var. *longispina* (P. Schulz) Schulz ex A. Bachmann.

Occurrence. Futoma 14, 16, 17, 18, Łubno 3.

Neonaviculopsis cf. ***eobiapiculata*** (Bukry) Desikachary & Prema (Fig. 2C)

Description. Single partial skeleton found has round-rectangular basal ring (at least 25.5 µm long in major axis) and at least one sharp apical spine (at least 8.3 µm long). Ring at least 13–15 µm wide in minor axis with basal sides slightly concave at point of arch attachment.

Notes. Basal ring length-to-width ratio (~2–3×) meets characteristics of *N. eobiapiculata*, especially the specimen shown by Bukry (1978b). As well, the preserved length of apical spine is close to half of the length of the basal ring. Three other similar species, *N. biapiculata* (Lemmermann) Frenguelli (in Desikachary & Prema 1996), *N. robusta* (Deflandre) Desikachary and Gowthaman (in Glezer 1970) and *N. quadrata* Ehrenberg show different proportions of the apical spine, basal ring length and width. These characters were emphasized as useful for taxonomic distinctions (Bukry 1978a). A few species included in the genus *Eunaviculopsis* (Desikachary & Prema 1996) include specimens with naviculoid outline of the basal ring and two portals, but skeletons are much larger than our specimen.

Occurrence. Futoma 14.

Neonaviculopsis sp. aff. ***N. neonautica*** (Bukry) Locker & Martini var. ***cocosensis*** (Bukry) Prema and Desikachary (Fig. 2D)

Description. Pear-shaped basal ring, 22–23 µm long in major and 12–15 µm in minor axis near cross-bridge attachment. Basal ring divided by central bridge into two unequal portals. Small apical basal spines and at least one pike at bridge-basal ring junction.

Notes. Skeletons with two portals are known among several genera, e.g., *Bachmannocena*, *Dictyocha*, and *Naviculopsis*. Some of the species in the *Bachmannocena diodon* (Ehrenberg) S. Locker group have been illustrated with two uneven portals (McCartney et al. 1995), noting that in some species the bridge may be positioned anywhere along the length of the basal ring (McCartney et al. 1995). In addition, not all these forms are symmetrical with respect to long and/or short axes. *Dictyocha* species [*D. brevispina* subsp. *ausomia* (Deflandre) Bukry, *D. navicula* Ehrenberg, *D. transenna* Bukry], *Corbisema cuspis* Busen and Wise, and several specimens designated as *Dictyocha* sp. naviculopsid-type have a generally broadly elliptical basal ring, relatively short basal spines, and symmetrical ring outline, in contrast to our specimens. Two-portal basal rings are also one of the diagnostic characters of the genus *Naviculopsis* and two other relatives established by Desikachary & Prema (1996), but in most species their rings are several times longer than they are wide and the basal spines are typically also significantly longer than those in the species of *Dictyocha/Bachmannocena* considered earlier. Our specimens do not conform well to the delineation of any species considered above. They differ from them by their smaller size and basal ring symmetry, being neither fusiform nor elliptical. They also possess at least one pike when none are mentioned in the original descriptions of those other species. The most shared morphological characters they have are with asymmetric skeletons of a species erected by Bukry (1981b) shown in Bukry (1981a) as *Dictyocha neonautica* var. *cococensis* currently included in the genus *Neonaviculopsis* established by Locker & Martini (1986).

Occurrence. Łubno 4.

Nucletmycea

Order: *Rotosphaerida*

Family: *Pompholyxophryidae*

Genus: *Pinaciophora*

Pinaciophora sp. (Fig. 4A)

Description. One fragment of a circular or elliptical structure recovered, at least 7.3 µm in diameter. Structure made of two layers, one with large circular openings (0.5–0.6 µm in diameter) overlaying a less perforated layer underneath. Openings concentrated in central part of structure and surrounded by a less perforated rim.

Notes. The most morphologically similar structures known to us are siliceous scales of rotosphaeridian heterotrophic and prymnesiophycean autotrophic protists. The rotosphaeridian cell covering elements (e.g., among members of the genus *Pinaciophora*) consist of two layers of siliceous sheeting. One of the layers is perforated by large, regularly dispersed openings, as seen in our specimen. However, reported scales are somewhat smaller than our specimen, generally less than 5 µm in diameter (Esteban et al. 2007; Bessudova et al. 2022).

In contrast, single-layer scales of the haptophyte *Hyalolithus*, particularly Mid-Eocene *Hyalolithus* aff. *tumescens* Abe, Tsutsui, and Jordan (Abe et al. 2016) and the late Eocene-early Oligocene specimens shown as *Pseudorocella barbadensis* Deflandre (Perch-Nielsen 1978) are closer in size to our specimen. However, these scales are elliptical when complete and exhibit a central elevation/depression undetectable in our admittedly fragmented specimen. Nonetheless, if our specimen represents a portion of an elliptical structure like a haptophyte scale mentioned above, it would better meet their size-range. The maximal diameter of our fragment fits well with the size and distribution of the openings of *H.* aff. *tumescens*, rather than the two other known species of the genus, *Hyalolithus didymus* Abe, Pellegrino, Lozar, Tsutsui and Jordan and *H. neolepis* Yoshida, Noël, Nakayama, Naganuma and Inouye (Abe et al. 2022), had they been single layered scales.

Occurrence. Łubno 4.

Genus: *Rabdiophrys*

cf. ***Rabdiophrys*** sp. (Fig. 4B)

Description. Circular scale made of two layers appearing to be joined peripherally. One layer contains a nearly circular structure with centrally located rimmed opening leading into chamber formed between the two layers. Scale diameter 4.5 µm, opening diameter 0.8–0.9 µm, rim 0.3–0.4 µm thick.

Notes. Plate scales covering the cells of *Rabdiophrys giraffensis* Siver and Skogstad, an unnamed member of the same genus (Siver & Lott 2023) and *Rabdiophrys* cf. *anulifera* Rainer emend. Siemensma (Bessudova et al. 2022) are similar to our specimen in gross morphology. However, our scale is larger than that of *Rabdiophrys* cf. *anulifera*, has a rimmed opening (unlike *Rabdiophrys* sp., Siver & Lott 2023) and is devoid of microperforations present in *R. giraffensis*. Our specimen therefore does not fit in the delineation of any of the three species. Interestingly, both *R. giraffensis* and *Rabdiophrys* sp. have been recovered from Eocene Arctic sediments and were the first fossil record of the genus. If related, our fossil would be only the third record worldwide and the first both from the Oligocene and outside the Arctic.

Occurrence. Borek Nowy Kawalec.

Eukarya Incertae Sedis

Some siliceous microfossils whose taxonomic affinity remains uncertain have traditionally been presented together with silicoflagellates, and so are included here.

Clathropyxidella sp. (Fig. 4C)

Description. Skeleton hemispherical, 4.8 µm in diameter, consisting of a polygonal net with at least 17 circular openings, 0.6–0.7 µm in diameter. Each opening rimmed with a shallow shelf.

Notes. Skeletons of *Clathropyxidella similis* Deflandre illustrated in Loeblich et al. (1968) and Perch-Nielsen (1978) are most structurally similar to our specimen. Those specimens are 7.0–9.0 µm in diameter and have 8–14 openings. Deflandre (1938, in Loeblich et al. 1968) described the species as a truncated sphere with a basal ring 7.0–8.5 µm in diameter, thus slightly less than the maximum diameter of the skeleton. A network of bars and openings is attached to the basal ring by 7–9 “pillars”. Owing to the position of our specimen, we cannot determine the number of pillars or the diameter of the basal ring.

There are semispherical/spherical silicoflagellate and ebridian species similar in gross morphology to our specimen and to *C. similis*. However, all are significantly larger than our specimen and the published documentation of specimens of *Clathropyxidella*. The structure of interconnecting bars of those skeletons is also different.

There are also several known species of silicoflagellates with a hemispherical apical apparatus over the basal ring with short basal spines. These are *Cannopilus jouseana* Bachmann, *C. sphericum* Geneinhold (50–60 µm in diameter), and *C. depressa* Locker in Locker & Martini (1986). Bukry & Monechi (1985) transferred some species from *Cannopilus* to *Caryocha*. Desikachary & Prema (1996) provide images and measurements of several of them including *C. depressa* and *C. jouseana*, with 30–40 µm diameter for the former, but no measurements

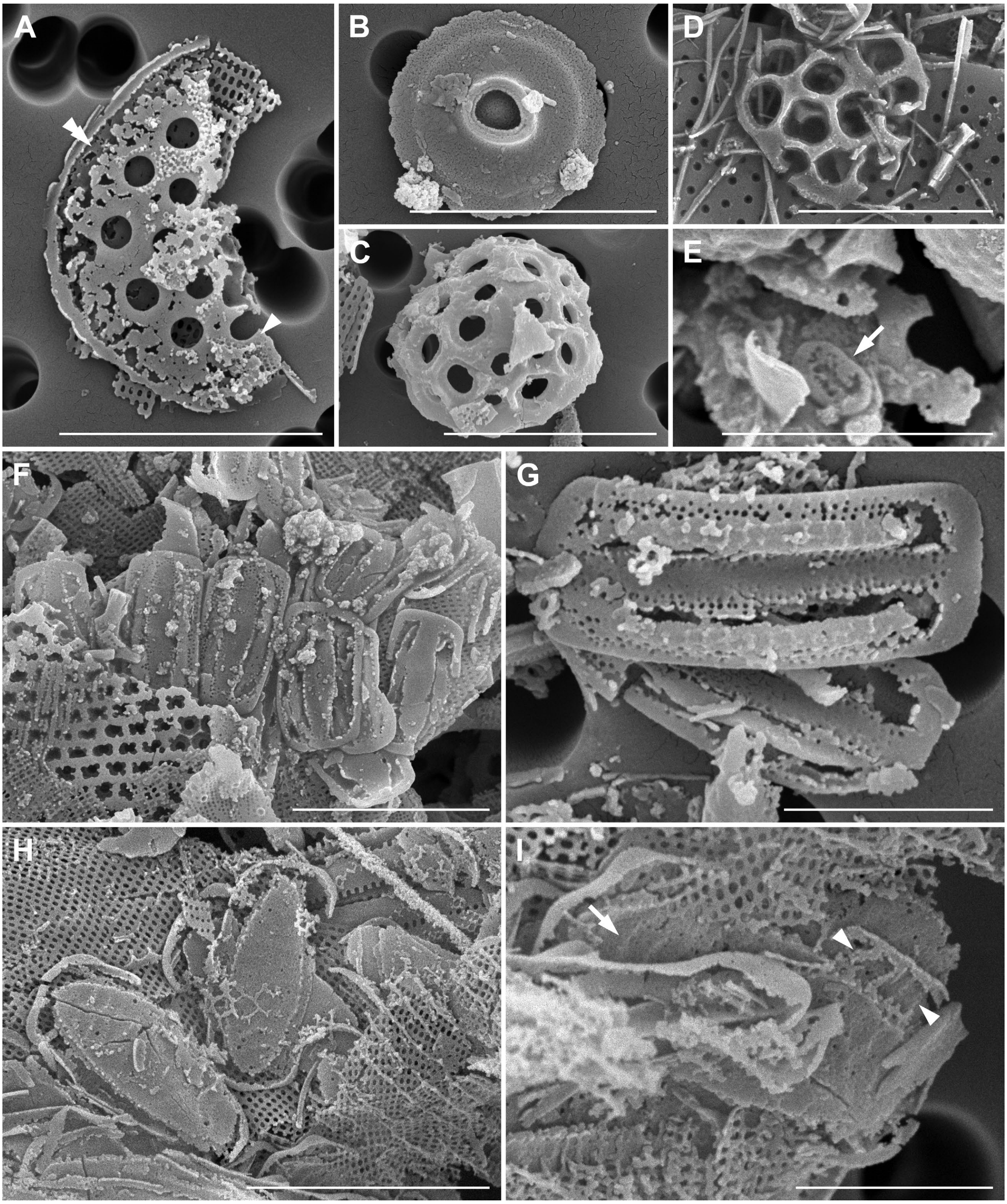

Figure 4. SEM images of scales. A – partial scale of *Pinaciophora* sp., note two layers connected to the marginal rim, single arrowhead points to top layer while double arrowhead points to bottom layer; B – scale of cf. *Rabdiophrys* sp., note bottom layer of two-layered scale is visible through central opening; C – subspherical skeleton of *Clathropyxidella* sp., note SEM preparation filter substrate visible through pores; D – slightly broken specimen of *Macrora* cf. *barbadensis*; E – small ellipsoidal scale (arrow) from an organism of uncertain affinity; F – group of overlapping rectangular scales in various degrees of preservation from an unknown organism; G – best-preserved scales from aggregate shown in Fig. 4F illustrate longitudinal fields of perforation; H – group of another type of scale, also from an unknown organism; I – close-up of one of the scales shown in Fig. 4H illustrating rippled central area (arrow) and ribs encircling scale center (arrowheads). Scales: A–F, H = 5 µm; G, I = 2 µm.

for the latter (neither magnification nor a scale bar are given for SEM images for these specimens). As well, some species in the genus *Distephanus* evolved an apical apparatus that renders them somewhat similar to *Carycocha*. They are *Distephanus speculum* var. *hemisphericum* Bukry and *D. xenus* Bukry. Their windows/portals, however, are polygonal, and the skeletons are approximately 24–30 µm in diameter. *Distephanus speculum* var. *hemisphericum* is a new combination and transfers specimens from other sources, with polygonal openings up to 7 per apical structure. All specimens of this taxon shown in McCartney & Wise (1990) and McCartney et al.

(1990) are larger and have basal spines, in contrast to our specimens.

Somewhat similar to our specimen in overall structure are also some of the small ebridians, such as *Pseudommodochium robustum* Deflandre, shown in Locker & Martini (1989), which are hemispherical with numerous openings (more than seen on our specimen), and diameter measured from the image is 21–25 µm, thus still much larger than our specimen. Diameters of *Pseudommodochium sphericum* Hovasse in Perch-Nielsen (1975) are 27.5–28.8 µm. All silicoflagellates and ebridians considered in comparison to our fossil are about an order of magnitude larger than our specimen.

Occurrence. Łubno 4.

Macrora cf. ***barbadensis*** (Deflandre) Bukry (Fig. 4D)

Description. Specimen is nearly circular and slightly domed, 5 µm in maximal linear dimension with slightly lobate margin and large polygonal openings (0.7–1.2 µm in diameter).

Notes. Our specimen does not fully conform to the delineation of any of three recognized species [*M. barbadensis*, *M. najae* Bukry, and *M. stella* (Azpeitia) Hanna]. It lacks a well-defined ring of larger marginal openings and is not as regularly circular as *M. stella* and *M. barbadensis*. A more irregular outline and distribution of openings are characteristic of *M. najae* (particularly that in Bukry 1977), but our specimen is less irregular than the published representatives of the species. Although our specimen shows some morphological affinity to *M. barbadensis* shown by Bukry (1977), it is smaller. Only Loeblich et al. (1968) and Fenner (1978) illustrate very small specimens (8.7 µm in diameter) with somewhat irregular outline and only a few openings like ours, yet under the name *Pseudorocella barbadensis* Deflandre. Perhaps the entire size range of *M. barbadensis* is not yet known.

Occurrence. Łubno 4.

Individual wall elements from organisms of uncertain affinity

Several morphological types of solitary scales or groups of scales were found. Owing to the chemical composition of the sediments (Kotlarczyk 1982) and preparatory treatment of the samples in which the scales were found (Kotlarczyk & Kaczmarska 1987), we presume that they all are siliceous.

Description. Individual scales from unknown organism rectangular or broadly elliptical, in overlapping aggregations similar to protistan cell coverings when seen in groups (Fig. 4F–H). Scale size variable, 1.7–5.3 µm in length and 1.0–2.2 µm in width. Most ornamented by perforation fields running along lateral margins, around entire margin, or at scale center. Morphotypes encountered are documented in Fig. 4E–I.

Notes. The overall structure of our scales differs from siliceous elements of wall coverings of the known extant chrysophytes (Cronberg 1986; Firsova et al. 2017; Siver & Lott 2017; Bessudova et al. 2022, 2023a, b) even though resting stages (stomatocysts) of presumptive chrysophytes are quite common in many of the samples examined here. They also differ from the few known siliceous scale bearing haptophytes (Yoshida et al. 2006), although a relatively small number of extant taxa of either alga has its entire set of cell covering elements examined in detail.

Scales covering cells are produced by a wide variety of extant protists, including ciliates, haptophytes, some rhizarians, testate lobose amoebas, chrysophytes, parmaphytes and green algae (Margulis et al. 1990), but our specimens do not conform to any extant scales known to us. Such scales are rarely preserved in the fossil record, although some exceptional ones (albeit non-siliceous) have been successfully recovered from sediments as old as the Neoproterozoic (Allison & Hilgert 1986; Cohen & Knoll 2012), yet none since. We document these structures here to bring attention to the significant diversity of fossilized micro- and nannofossils, even though their phylogenetic placement remains uncertain.

Occurrence. Borek Nowy Dom 5, Borek Nowy Kawalec, Łubno 4.

Discussion

Relatively low species diversity in silicoflagellates and their delicate skeletons cause them to be preserved infrequently in marine sediments, both in past and extant seafloors (McCartney 1993; Martínez-López et al. 2016). The Early Oligocene was a particularly tumultuous time both globally and in the region of the Central Paratethys which contributed to the poor fossil record of the resident biota. Here, for the first time silicoflagellates are documented as found in the Central Paratethys. The specimens we document are those that were recovered in a state of preservation allowing a degree of confidence in their identification. In addition, in many other samples we found a great number of fragments of *Corbisema* and *Dictyocha*-like skeletons that were too small to identify. This suggests a greater number of specimens and perhaps species than appear from our presentation.

Compared to reports from sites of similar age from the Southern Hemisphere, our silicoflagellate assemblage is relatively species poor. Up to 20–35 taxa were found in Oligocene cores from Antarctic, subantarctic Atlantic and Pacific Oceans (Ciesielski 1975; Shaw & Ciesielski 1983; Bukry 1991; McCartney et al. 2023). Recovered silicoflagellate floras from the Northern Hemisphere are generally less species-rich and more in line with the number of taxa we report. Late Eocene – Early Oligocene flora of the Bering Sea include 18 species while Oligocene sections from the Norwegian and Greenland Seas yielded a similar number, ~10–14 species (Ling 1985; Bukry 1976b; Martini & Müller 1976). The Norwegian and Greenland Seas were relatively less connected to the world's largest, warmer water oceans of that time. Thus, when compared to Indo-Pacific sites thus far examined, the northern seas fossil assemblages recovered were not unlike the Early Oligocene region of the central Paratethys. Therefore, it should not be surprising that in the farther southeast located Donbas (Olshtynska 2013) and Azov regions (Olshtynska & Tsoy 2018) the silicoflagellate flora was more diverse. Twenty and twenty-eight taxa were found in sediments straddling the late Eocene and early Oligocene of the Eastern Paratethys, respectively, more in line with those documented from the Southern Hemisphere.

Because the age of the sediments examined here is now well established (Kotlarczyk et al. 2006; Kotlarczyk & Uchman 2012), their biostratigraphy was not the goal of our investigations. Nonetheless, we observe that some of the species found in our samples are known to be widely distributed both temporally and spatially. For example, *Corbisema apiculata*, *C. triacantha*, *Dictyocha fibula*, and *Distephanopsis crux* are distributed widely from the Cretaceous to Recent. A few others have been known from more restricted time intervals or geographies. *Dictyocha deflandrei* and *Neonaviculopsis eobiapiculata* are reported from the Paleocene to Late Oligocene (Ciesielski 1975; Hajós 1976; possibly Bukry 1976b; Shaw & Ciesielski 1983; Desikachary & Prema 1996; McCartney et al. 2023), although the former more commonly in southern than northern paleo-oceans. Finally, we also found species which had previously been reported from sediments younger than Rupelian. *Corbisema triacantha* var. *nuda* is thus far known only from the original, Middle Miocene site in the southern North Atlantic (Bukry 1982). It is uncertain what prevailing factors were responsible for low species diversity in our samples. Both geological (tectonic unrest, terrestrial sediment load; Kotlarczyk et al. 2006) and paleoceanographic (Hutchinson et al. 2021; Palcu & Krijgsman 2023) factors could have contributed or were responsible for the low species diversity and/or state of skeleton preservation.

Although their taxonomic affinity remains uncertain, the diversity of non-silicoflagellate siliceous micro- and nannofossils found in our samples is quite high when compared to many published micropaleontological reports. To some extent, this may be due to the methods of sample processing used by some researchers (e.g., involving sediment sieving and only light microscopy) and/or simple underreporting. However, a few of those recovering fossils in the 10 µm or less size range have proven particularly informative and helpful (Abe et al. 2016, 2022; Siver 2020; Siver & Skogstad 2021; Siver & Lott 2023). Hopefully, those reports along with ours will stimulate interest in continuing such examinations in the future. We underscore the benefits and significance for micropaleontological studies of the use of scanning electron microscopy and methods of preparation that are conducive to recovery of micro- and nannofossils in sedimentary samples.

Acknowledgements

We thank K. Wołowski of the Department of Phycology, as well as the Directors of the Polish Academy of Sciences (PAS) Institute of Botany for making this material available to us. The late J. Kotlarczyk of the Academy of Mining and Metallurgy (AGH) in Kraków led field expeditions. Funding for field work, sample processing and early analyses in the mid- to late 1970s was provided by the AGH and PAS in Kraków and the Polish Geological Institute in Warsaw. We appreciate help of the late J. Piątek in processing the sediment samples. We are also grateful for the constructive comments of two anonymous reviewers that greatly improved the publication. Funding for electron microscopy of siliceous microfossils was provided by an NSERC Discovery Grant and the Mount Allison University Marjorie Bell Faculty Fund (Sabbatical) awarded to IK.

References

Abe, K., McCartney, K., Fukunaga, Y., Narita, H. & Jordan, R. W. 2015. Silicoflagellates and ebridians from the Seto Inland Sea and Kuroshio, including the description of *Octactis pulchra* var. *takahashii* var. nov. *Journal of Nannoplankton Research* 35: 111–128. https://doi.org/10.58998/jnr2001

Abe, K., Tsutsui, H. & Jordan, R. W. 2016. *Hyalolithus tumescens* sp. nov., a siliceous scale-bearing haptophyte from the middle Eocene. *Journal of Micropalaeontology* 35: 143–149.

Abe, K., Pellegrino, L., Lozar, F., Tsutsui, H. & Jordan, R. W. 2022. *Hyalolithus didymus* sp. nov. (*Haptophyta*): a late Miocene siliceous microfossil from Sicily, Italy. *Phycologia* 61: 504–513. https://doi.org/10.1080/00318884.2022.2080996

Allison, C. W. & Hilgert, J. W. 1986. Scale microfossils from the Early Cambrian of Northwest Canada. *Journal of Paleontology* 60: 973–1015. https://doi.org/10.1017/S0022336000022538

Barron, J. A., Bukry, D. & Poore, R. Z. 1984. Correlation of the middle Eocene Kellogg Shale of northern California. *Micropaleontology* 30: 138–170. https://doi.org/10.2307/1485715

Bessudova, A. Y., Firsova, A. D. & Likhoshway, Y. V. 2022. Silica-scaled heterotrophic protists Rotosphaerida, Thaumatomonadida, and Centroplasthelida in the large continuous ecosystem connecting Lake Baikal to the Kara Sea. *The Journal of Eukaryotic Microbiology* 69: e12871. https://doi.org/10.1111/jeu.12871

Bessudova, A. Y., Firsova, A. D., Bukin, Y., Kopyrina, L., Zakharova, Y. & Likhoshway, Y. V. 2023a. Under-ice development of silica-scaled chrysophytes with different trophic mode in two ultraoligotrophic lakes of Yakutia. *Diversity* 15: 326. https://doi.org/10.3390/d15030326

Bessudova, A. Y., Likhoshway, Y. V., Firsova, A. D., Mitrofanova, E., Koveshnikov, M., Soromotin, A., Khoroshavin, V. & Kirillov, V. 2023b. Small organisms in a large river: What provides the high diversity of scaled chrysophytes in the Ob River? *Water* 15: 3054. https://doi.org/10.3390/w15173054

Bukry, D. 1975a. Silicoflagellate and coccolith stratigraphy, Deep Sea Drilling Project, Leg 29. *Initial Reports of the Deep Sea Drilling Project* 29: 845–872.

Bukry, D. 1975b. Coccolith and silicoflagellate stratigraphy, northwestern Pacific Ocean, Deep Sea Drilling Project, Leg 32. *Initial Reports of the Deep Sea Drilling Project* 32: 677–701.

Bukry, D. 1976a. Cenozoic silicoflagellate and coccolith stratigraphy, South Atlantic Ocean, Deep Sea Drilling Project Leg 36. *Initial Reports of the Deep Sea Drilling Project* 35: 885–917.

Bukry, D. 1976b. Silicoflagellate and coccolith stratigraphy, Norwegian-Greenland Sea, Deep Sea Drilling Project Leg 38. *Initial Reports of the Deep Sea Drilling Project* 38: 843–855.

Bukry, D. 1976c. Silicoflagellate and coccolith stratigraphy, southeastern Pacific Ocean, Deep Sea Drilling Project Leg 34. *Initial Reports of the Deep Sea Drilling Project* 34: 715–735.

Bukry, D. 1977. Coccolith and silicoflagellate stratigraphy, South Atlantic Ocean, Deep Sea Drilling Project Leg 39. *Initial Reports of the Deep Sea Drilling Project* 39: 825–839.

Bukry, D. 1978a. Cenozoic silicoflagellate and coccolith stratigraphy, northwestern Atlantic Ocean, Deep Sea Drilling Project Leg 43. *Initial Reports of the Deep Sea Drilling Project* 44: 775–805.

Bukry, D. 1978b. Cenozoic coccolith, silicoflagellate, and diatom stratigraphy, Deep Sea Drilling Project Leg 44. *Initial Reports of the Deep Sea Drilling Project* 44: 807–863.

Bukry, D. 1980. Silicoflagellate biostratigraphy and paleoecology in the eastern Equatorial Pacific, Deep Sea Drilling Project Leg 54. *Initial Reports of the Deep Sea Drilling Project* 54: 545–573.

Bukry, D. 1981a. Silicoflagellate stratigraphy of offshore California and Baja California, Deep Sea Drilling Project Leg 63. *Initial Reports of the Deep Sea Drilling Project* 63: 539–557.

Bukry, D. 1981b. Synthesis of silicoflagellate stratigraphy from Maestrichtian to Quaternary marine sediment. *Society for Sedimentary Geology Special Publication* 32: 433–444. https://doi.org/10.2110/pec.81.32.0433

Bukry, D. 1982. Cenozoic silicoflagellates from offshore Guatemala, Deep Sea Drilling Project Site 495. *Initial Reports of the Deep Sea Drilling Project* 67: 425–445.

Bukry, D. 1983. Upper Cenozoic silicoflagellates from offshore Ecuador, Deep Sea Drilling Project Sit 504. *Initial Reports of the Deep Sea Drilling Project* 69: 321–342.

Bukry, D. 1991. Oligocene and Quaternary silicoflagellates from the Kerguelen Plateau. *Proceedings of the Ocean Drilling Program, Scientific Results* 119: 933–934.

Bukry, D. & Foster, J. H. 1973. Silicoflagellate and diatom stratigraphy, Leg 16, Deep Sea Drilling Project *Initial Reports of the Deep Sea Drilling Project* 16: 815–871.

Bukry, D. & Monechi, S. 1985. Late Cenozoic silicoflagellates from the northwest Pacific, Deep Sea Drilling Project Leg 86: Paleotemperature trends and texture classification. *Initial Reports of the Deep Sea Drilling Project* 86: 367–397.

Burki, F. 2014. The eukaryotic tree of life from a global phylogenomic perspective. *Cold Spring Harbor Perspectives in Biology* 6: a016147. https://doi.org/10.1101/cshperspect.a016147

Chang, F. H., Sutherland, J. & Bradford-Grieve, J. 2017. Taxonomic revision of *Dictyochales* (*Dictyochophyceae*) based on morphological, ultrastructural, biochemical and molecular data. *Phycological Research* 65: 235–247. https://doi.org/10.1111/pre.12181

Ciesielski, P. F. 1975. Biostratigraphy and paleoecology of Neogene and Oligocene silicoflagellates from cores recovered during Antarctic Leg 28, Deep Sea Drilling Project. *Initial Reports of the Deep Sea Drilling Project* 28: 625–691.

Cohen, P. A. & Knoll, A. H. 2012. Scale microfossils from the Mid-Neoproterozoic Fifteenmile Group, Yukon Territory. *Journal of Paleontology* 86: 775–800. https://doi.org/10.1666/11-138.1

Cronberg, G. 1986. Chrysophycean cysts and scales in lake sediments: a review. In: Kristiansen, J. & Andersen, R. A. (eds), *Chrysophytes: Aspects and Problems*, pp. 281–315. Cambridge University Press, Cambridge.

Derelle, R., López-García, P., Timpano, H. & Moreira, D. 2016. A phylogenomic framework to study the diversity and evolution of stramenopiles (=heterokonts). *Molecular Biology and Evolution* 33: 2890–2898. https://doi.org/10.1093/molbev/msw168

Desikachary, T. V. & Prema, P. 1996. *Silicoflagellates (Dictyochophyceae)*. J. Cramer, Berlin.

Dumitrică, P. 1978. Badenian silicoflagellates from Central Paratethys. In: Brestenská, E. (ed.), *Chronostratigraphie und Neostratotypen, Miozän der Zentralen Paratethys*, pp. 207–227. Veda, Bratislava.

Esteban, G. F., Gooday, A. J. & Clarke, K. J. 2007. Siliceous scales of filose-amoebae (*Pompholyxophryidae*, Rotosphaerida) from deep Southern Ocean sediments, including first records for the Southern Hemisphere. *Polar Biology* 30: 945–950. https://doi.org/10.1007/s00300-007-0280-4

Fenner, J. 1978. Cenozoic diatom biostratigraphy of the equatorial and southern Atlantic Ocean. *Initial Reports of the Deep Sea Drilling Project* 39: 491–624.

Firsova, A. D., Bessudova, A. Y. & Likhoshway, Y. V. 2017. New data of chrysophycean stomatocysts from Lake Baikal. *Acta Biologica Sibirica* 3: 113–122.

Glezer, Z. I. 1970. *Cryptogamic Plants of the USSR. Volume VII. Silicoflagellatophyceae*. Israel Program for Scientific Translations for the National Science Foundation, Washington D.C.

Graham, J. E., Wilcox, L. W. & Graham, L. E. 2008. *Algae (2nd edition)*. Benjamin Cummings, San Francisco.

Hajós, M. 1976. Upper Eocene and Lower Oligocene *Diatomaceae*, *Archaeomonadaceae*, and Silicoflagellatae in southwestern Pacific sediments, DSDP Leg 29. *Initial Reports of the Deep Sea Drilling Project* 35: 817–883.

Haq, B. U. 1998. Silicoflagellates and ebridians. In: Haq, B. U. & Boersma, A. (eds), *Introduction to Marine Micropaleontology*, pp. 267–275. Elsevier, Amsterdam.

Hutchinson, D. K., Coxall, H. K., Lunt, D. J., Steinthorsdottir, M., de Boer, A. M., Baatsen, M., von der Heydt, A., Huber, M., Kennedy-Asser, A. T., Kunzmann, L., Ladant, J.-B., Lear, C. H., Moraweck, K., Pearson, P. N., Piga, E., Pound, M. J., Salzmann, U., Scher, H. D., Sijp, W. P., Śliwińska, K. K., Wilson, P. A. & Zhang, Z. 2021. The Eocene-Oligocene transition: A review of marine and terrestrial proxy data, models and model-data comparisons. *Climate of the Past* 17: 269–315. https://doi.org/10.5194/cp-17-269-2021

Ichikawa, W., Shimizu, I. & Bachmann, A. 1967. Fossil silicoflagellates and their associated uncertain forms in Iida Diatomite, Noto Peninsula, Central Japan. *Science Reports of the Kanazawa University* 12: 143–172.

Jordan, R. W. & McCartney, K. 2015. *Stephanocha* nom. nov., a replacement name for the illegitimate silicoflagellate genus *Distephanus* (*Dictyophyceae*). *Phytotaxa* 201: 177–187. https://doi.org/10.11646/phytotaxa.201.3.1

Kaczmarska, I. 1982. Diatoms of the two Lower Oligocene diatomites from the Polish Carpathian Flysch. *Acta Geologica Academiae Scientiarum Hungaricae* 25: 39–47.

Kaczmarska, I. & Ehrman, J. M. 2008. *Poloniasira fryxelliana* Kaczmarska and Ehrman, a new thalassiosiroid diatom (*Bacillariophyta*) from the Lower Oligocene diatomites in Polish Flysch Carpathians, southeast Poland. *Nova Hedwigia, Beihefte* 133: 217–230.

Kaczmarska, I. & Ehrman, J. M. 2023. Parmalean and other siliceous nannofossils from the Oligocene Polish Flysch Carpathians. *Acta Palaeontologica Polonica* 68: 441–456. https://doi.org/10.4202/app.01078.2023

Kotlarczyk, J. 1982. Role of diatoms in sedimentation and biostratigraphy of the Polish Flysch Carpathians. *Acta Geologica Academiae Scientiarum Hungaricae* 25: 9–21.

Kotlarczyk, J., Jerzmańska, A., Świdnicka, E. & Wiszniowska, T. 2006. A framework of ichthyofaunal stratigraphy of the Oligocene-Early Miocene strata of the Polish Outer Carpathian Basin. *Annales Societatis Geologorum Poloniae* 76: 1–111.

Kotlarczyk, J. & Kaczmarska, I. 1987. The two horizons with the Oligocene and Lower Miocene diatoms from the Polish Outer Carpathians. *Annales Societatis Geologorum Poloniae* 57: 143–189.

Kotlarczyk, J. & Lesniak, T. 1990. *Lower Part of the Menilite Formation and Related Futoma Diatomite Member in the Skole Unit of the Polish Carpathians.* Wydawnictwo Akademii Góniczo-Hutniczej, Kraków.

Kotlarczyk, J. & Uchman, A. 2012. Integrated ichnology and ichthyology of the Oligocene Menilite Formation, Skole and Subsilesian nappes, Polish Carpathians: a proxy to oxygenation history. *Palaeogeography, Palaeoclimatology, Palaeoecology* 331–332: 104–118. https://doi.org/10.1016/j.palaeo.2012.03.002

Ling, H. Y. 1985. Paleogene silicoflagellates and ebridians from the Goban Spur, northeastern Atlantic. *Initial Reports of the Deep Sea Drilling Project* 80: 663–668.

Locker, S. & Martini, E. 1986. Silicoflagellates and some sponge spicules from the southwest Pacific, Deep Sea Drilling Project, Leg 90. *Initial Reports of the Deep Sea Drilling Project* 90: 887–924.

Locker, S. & Martini, E. 1989. Cenozoic silicoflagellates, ebridians, and actiniscidians from the Vøring Plateau (ODP Leg 104). *Proceedings of the Ocean Drilling Program, Scientific Results* 104: 543–585.

Loeblich III, A. R., Loeblich, L. A., Tappan, H. & Loeblich Jr., A. R. 1968. *Annotated Index of Fossil and Recent Silicoflagellates and Ebridians with Descriptions and Illustrations of Validly Proposed Taxa*. The Geological Survey of America, Boulder.

Lozar, F. & Mussa, M. 2003. Silicoflagellate biostratigraphy, Hole 1149A (ODP Leg 185, Nadezhda Basin, Northwestern Pacific). *Proceedings of the Ocean Drilling Program, Scientific Results* 185: 1–18.

Margulis, L., Corliss, J. O., Melkonian, M. & Chapman, D. J., eds 1990. *Handbook of Protoctista*. Jones and Bartlett, Boston.

Martínez-López, A., Álvarez-Gómez, I. G., Pérez-Cruz, L., Verdugo-Díaz, G. & Villegas-Aguilera, M. M., 2016. Production, exportation and preservation of silicoflagellates in Alfonso Basin, Gulf of California. *Journal of Sea Research* 109: 52–-62. https://doi.org/10.1016/j.seares.2016.01.005

Martini, E. 1982. Pliocene and Quaternary diatoms, silicoflagellates, sponge spicules, and endoskeletal dinoflagellates from the Philippine Sea, Deep Sea Drilling Project Legs 59 and 60. *Initial Reports of the Deep Sea Drilling Project* 60: 565–574.

Martini, E. 1990. Tertiary and Quaternary silicoflagellates, actiniscidians, and ebridians from the Eastern Pacific off Peru (Leg 112). *Proceedings of the Ocean Drilling Program, Scientific Results* 112: 157–173.

Martini, E. & Müller, C. 1976. Eocene to Pleistocene silicoflagellates from the Norwegian-Greenland Sea (DSDP Leg 38). *Initial Reports of the Deep Sea Drilling Project* 38: 857–895.

McCartney, K. 1993. Silicoflagellates. In: Lipps, J. H. (ed.), *Fossil prokaryotes and protists*, pp. 143–154. Blackwell Scientific Publications, Oxford.

McCartney, K. & Wise Jr., S. W. 1987. Silicoflagellates and ebridians from the New Jersey Transect, Deep Sea Drilling Project Leg 93, Sites 604 and 605. *Initial Reports of the Deep Sea Drilling Project* 93: 801–814.

McCartney, K. & Wise Jr., S. W. 1990. Cenozoic silicoflagellates and ebridians from ODP Leg 113: biostratigraphy and notes on morphologic variability. *Proceedings of the Ocean Drilling Program, Scientific Results* 113: 729–760.

McCartney, K. & Witkowski, J. 2016. Cenozoic silicoflagellate skeletal morphology: a review and suggested terminology. *Journal of Micropalaeontology* 35: 179–189. https://doi.org/10.1144/jmpaleo2015-018

McCartney, K., Wise Jr., S. W., Harwood, D. M. & Gersonde, R. 1990. Enigmatic Lower Albian silicoflagellates from ODP Site 693: Progenitors of the order Silicoflagellata? *Proceedings of the Ocean Drilling Program, Scientific Results* 113: 427–442.

McCartney, K., Churchill, S. & Woestendiek, L. 1995. Silicoflagellates and ebridians from Leg 138, eastern equatorial Pacific. *Proceedings of the Ocean Drilling Program, Scientific Results* 138: 129–162.

McCartney, K., Witkowski, J. & Harwood, D. M. 2010. Early evolution of the silicoflagellates during the Cretaceous. *Marine Micropaleontology* 77: 83–100. http://dx.doi.org/10.1016/j.marmicro.2010.08.001

McCartney, K., Witkowski, J., Jordan, R. W., Abe, K., Januszkiewicz, A., Wrobel, R., Bak, M., & Soeding, E. 2022. Silicoflagellate evolution through the Cenozoic. *Marine Micropaleontology* 172: 1–18. https://doi.org/10.1016/j.marmicro.2022.102108

McCartney, K., Chakraborty, A., Ghosh, A. K., Soeding, E. & Rout, V. 2023. Diversity and evolution of late Eocene to late Oligocene silicoflagellates from IODP Expedition 378 Holes U1553A and U1553B, southwest Pacific Ocean. *Marine Micropaleontology* 179: 102215. https://doi.org/10.1016/j.marmicro.2023.102215

Olshtynska, O. P. 2013. Eocene and Early Oligocene silicoflagellates and ebridians from the Ukraine. *Collection of Scientific Works of the Institute of Geological Sciences of the NAS of Ukraine* 6: 131–135.

Olshtynska, O. P. & Tsoy, I. 2018. Silicoflagellates of the Late Eocene to Early Oligocene of Eastern Paratethys (Azov Sea area of Ukraine). *Nova Hedwigia, Beihefte* 147: 141–150.

Onodera, J. & Takahashi, K. 2009. Taxonomy and biostratigraphy of middle Eocene silicoflagellates in the central Arctic Basin. *Micropaleontology* 55: 209–248.

Palcu, D. V. & Krijgsman, W. 2023. The dire straits of Paratethys: gateways to the anoxic giant of Eurasia. *Geological Society of London Special Publications* 523: 111. https://doi.org/10.1144/sp523-2021-73

Perch-Nielsen, K. 1975. Late Cretaceous to Pleistocene silicoflagellates from the southern southwest Pacific, DSDP, Leg 29. *Initial Reports of the Deep Sea Drilling Project* 29: 677–721.

Perch-Nielsen, K. 1978. Eocene to Pliocene archaeomonads, ebridians, and endoskeletal dinoflagellates from the Norwegian Sea, DSDP Leg 38. *Initial Reports of the Deep Sea Drilling Project* 38-41 Supplement: 147–175.

Picha, F. J. & Stranik, Z. 1999. Late Cretaceous to early Miocene deposits of the Carpathian foreland basin in southern Moravia. *International Journal of Earth Sciences* 88: 475–495. https://doi.org/10.1007/s005310050280

Sachsenhofer, R. F., Popov, S. V., Bechtel, A., Coric, S., Francu, J., Gratzer, R., Grunert, P., Kotarba, M., Mayer, J., Pupp, M., Rupprecht, B. J. & Vincent, S. J. 2017. Oligocene and Lower Miocene source rocks in the Paratethys: Palaeogeographical and stratigraphic controls. In: Simmons, M. D., Tari, G. C. & Okay, A. I. (eds), *Petroleum Geology of the Black Sea – Geological Society of London Special Publications*, pp. 267–306.

Schellpeper, M. E. & Watkins, D. K. 1998. Oligocene to Early Miocene silicoflagellates from the Ivorian Basin, eastern equatorial Atlantic, Site 959. *Proceedings of the Ocean Drilling Program, Scientific Results* 159: 493–508.

Shaw, C. A. & Ciesielski, P. F. 1983. Silicoflagellate biostratigraphy of Middle Eocene to Holocene Subantarctic sediments recovered by Deep Sea Drilling Project Leg 71. *Initial Reports of the Deep Sea Drilling Project* 71: 687–737.

Siver, P. A. 2020. Remarkably preserved cysts of the extinct synurophyte, *Mallomonas ampla*, uncovered from a 48 Ma freshwater Eocene lake. *Scientific Reports* 10: 5204. https://doi.org/10.1038/s41598-020-61993-1

Siver, P. A. & Lott, A. M. 2017. The scaled chrysophyte flora in freshwater ponds and lakes from Newfoundland, Canada, and their relationship to environmental variables. *Cryptogamie Algologie* 38: 325–347. http://dx.doi.org/10.7872/crya/v38.iss4.2017.325

Siver, P. A. & Lott, A. M. 2023. History of the Giraffe Pipe locality inferred from microfossil remains: A thriving freshwater ecosystem near the Arctic Circle during the warm Eocene. *Journal of Paleontology* 97: 271–291. https://doi.org/10.1017/jpa.2022.101

Siver, P. A. & Skogstad, A. 2021. A first account of the heterotrophic eukaryote *Rabdiophrys* Rainer from the fossil record and description of a new species from an ancient Eocene Arctic freshwater lake. *European Journal of Protistology* 82: 125857. https://doi.org/10.1016/j.ejop.2021.125857

Strassert, J. F. H., Irisarri, I., Williams, T. A. & Burki, F. 2021. A molecular timescale for eukaryote evolution with implications for the origin of red algal-derived plastids. *Nature Communications* 12: 1879. https://doi.org/10.1038/s41467-021-22044-z

Strassert, J. F. H., Jamy, M., Mylnikov, A. P., Tikhonenkov, D. V. & Burki, F. 2019. New phylogenomic analysis of the enigmatic phylum Telonemia further resolves the eukaryote tree of life. *Molecular Biology and Evolution* 36: 757–765. https://doi.org/10.1093/molbev/msz012

Tikhonenkov, D. V., Jamy, M., Borodina, A. S., Belyaev, A. O., Zagumyonnyi, D. G., Prokina, K. I., Mylnikov, A. P., Burki, F.

& Karpov, S. A. 2022. On the origin of TSAR: Morphology, diversity and phylogeny of Telonemia. *Open Biology* 12: 210325. https://doi.org/10.1098/rsob.210325

Tsutsui, H., Jordan, R. W., Nishiwaki, N. & Nishida, S. 2018. Morphometric analysis of early Eocene *Corbisema* skeletons (Silicoflagellata) in Mors, Denmark. *Journal of Micropalaeontology* 37: 283–293. https://doi.org/10.5194/jm-37-283-2018

Van den Hoek, C., Mann, D. G., & Jahns, H. M. 1995. *Algae: an Introduction to Phycology*. Cambridge University Press, Cambridge.

Yoshida, M., Noël, M.-H., Nakayama, T., Naganuma, T. & Inouye, I. 2006. A haptophyte bearing siliceous scales: Ultrastructure and phylogenetic position of *Hyalolithus neolepsis* gen. et sp. nov. (*Prymnesiophyceae*, *Haptophyta*). *Protist* 157: 213–234. https://doi.org/10.1016/j.protis.2006.02.004